

MODELS FOR BROAD AREA EVENT IDENTIFICATION AND YIELD ESTIMATION: MULTIPLE CODA TYPES

W. Scott Phillips, Hans E. Hartse, George E. Randall, Richard J. Stead, Michael L. Begnaud, and Dale N. Anderson

Los Alamos National Laboratory

Sponsored by the National Nuclear Security Administration

Award No. DE-AC52-06NA25396/LA10-Yield-NDD02/LA10-ECM-NDD02

ABSTRACT

Models of laterally varying attenuation and site effects of regional phases and their codas are necessary to correct regional amplitudes to reveal source effects of importance to identification and yield estimation procedures. We accomplish this using 2-D amplitude tomography, incorporating absolute spectral estimates based on precise ratio techniques and moment tensor results. The spectral constraints allow calibration to absolute levels, and can be used to validate amplitude prediction models. Constraints may also be used to improve resolution in the margins of raypath coverage where source-path tradeoffs would otherwise dominate.

Our recent efforts have focused on improving coda analysis in areas of low Q and blockage. We must be able to use whatever coda type appears in our records if we are to estimate Mw for MDAC purposes, or use in yield estimation studies. The Lg coda has been used the most in such studies; however low crustal Q can strip the Lg and its coda from the record, especially at long distances and high frequencies. We often observe high quality Pn and Sn coda in such cases. Pg coda is observed for close in recordings, and behaves similarly to the Lg, with strength in lower bands, but generally has limited application outside local distance ranges. We have examined coda envelopes in plate boundary regions of Asia that are known to severely attenuate Lg, picking Pn, Pg, Sn, and Lg coda manually. We then processed coda using standard methods before turning amplitude data over to a simultaneous inversion of multi-coda type and multi-band data for 2-D path effects, site effects, and the absolute transfer function. The multiple coda types improved the bandwidths of observed seismic spectra as Lg covered low frequencies, and Pn and Sn coda covered overlapping high frequency bands, with the Pn band slightly higher than the Sn band. Distances were too great to include Pg coda in this study. Residuals show that path models fit Lg coda data to 0.10 – 0.18 log₁₀ units, varying with band, Sn coda to 0.14 – 0.20, and similarly for Pn. Pn direct phase amplitudes normally display higher scatter than other regional phases, the improved behavior in this case may be due to the coda measurement or to a limited source region compared to other studies.

OBJECTIVES

We seek models that will allow the prediction of absolute spectral levels from regional phase direct and coda phases, for purposes of event identification and yield estimation. Models can be constrained and validated using absolute spectra obtained using relative amplitude techniques, with overall levels set by moment tensor studies. Spectral constraints are used to break source-path (corner frequency-Q) tradeoffs, allowing extension of models into poorly covered regions, and can be used for model validation as is done for velocity models using location ground truth. Models will allow the isolation of near-source effects on explosion spectra, and the evaluation of test site biases, thus enable transportable, regional phase yield estimation.

RESEARCH ACCOMPLISHED

Attenuation models are critical for magnitude and yield work (e.g., Nuttli, 1973) and benefit event identification studies through the reduction of discriminant scatter for distributions of earthquakes across large areas. Phillips et al. (1998) showed that 2-D empirical path correction for 0.5-8 Hz Pn, Pg, Sn and Lg phases reduced discriminant scatter in earthquake populations in China, especially for lower and intermediate bands (0.5-6 Hz). The effect in intermediate bands (2-6 Hz) is of particular importance as discrimination performance degrades toward low frequency (Walter et al., 1995; Taylor 1996). Discrimination is known to perform well in high bands (> 6 Hz), but signal-to-noise considerations limit the range at which those bands are observed. Thus, intermediate band discrimination is of importance in extending discrimination to smaller events and larger distances.

Tomographic models are superior to empirical models as attenuation can be constrained in areas without reference events, but that are crossed by raypaths from outside events. The Los Alamos team has been active in producing such models using a wide range of techniques (Phillips et al., 2000, 2005, 2008; Phillips and Stead, 2008), including dual-phase tomography (Phillips et al., 2001), Bayesian approaches (Taylor et al., 2003), accounting for left censored amplitude data (Taylor et al., 2003), and spherical earth spreading models for Pn (Yang et al., 2007). This has and continues to be an active area of research in the community as well (e.g., Campillo, 1987; Jin and Aki, 1988; Xie et al., 2006; Mitchell et al., 1997; Pei et al., 2006; Mayeda et al., 2005; Ford et al., 2009; Pasyanos et al., 2009).

Activity this year has primarily focused on multiple coda types, but has also included significant improvements to noise analysis techniques for identifying suspicious instrument intervals, such as undocumented gain shifts, and to simultaneous multi-band inversion for peak envelope and coda shape models.

We have used sequences of pre-event noise to identify suspicious data intervals in past work (e.g. Phillips et al., 2008), but have recently tested simple methods that find the minimum noise level for a series of nighttime measurements made every possible night without regard to the event data set. This method provides much cleaner noise sequences when continuous data are available, as it avoids diurnal variations, improving our ability to identify suspicious time intervals. Figure 1 shows results for stations AAK and KMI. Seasonal variations are very clear, as is the increasing trend at KMI, which is typical of much of the CDSN. We mark suspicious intervals and do not use those data for amplitude studies pending closer review. To date, we have logged 2334 suspicious high frequency noise intervals (1-2 Hz and 4-8 Hz) for multiple channels of 1287 eastern Eurasia stations.

Our envelope peak and coda shape models rely on robust data binning over distance intervals, to which model parameters are fit simultaneously for all bands. L1 binning and stacking reduces the effects of outliers and produce smaller data sets that can be used with faster L2 inversion procedures. Median coda stacks are shown for 2-3 Hz Pn, Sn, and Lg coda in Figure 2, along with model fits. These models are used to measure coda amplitudes from envelope data.

Our coda path inversion is done simultaneously for multi-band and multi-coda type data, as described for a direct wave study by Phillips et al. (2010). We used constraints from regional moments, most from the literature, and spectra computed using relative direct and coda measurements of event cluster data (Figure 3). Spreading is fixed for each phase and band and inversion is performed for 2-D Q, site effects, and absolute transfer function, all dependent on phase and band, and source effects, only dependent on band. Sources are modeled using the MDAC formulation (Walter and Taylor, 2002), with no constraint on source corner frequency (or apparent stress), other than a similarity constraint for poorly resolved, i.e. flat, spectra (Fehler and Phillips, 1991). We restricted this inversion to earthquake sources, but the code is designed to include explosions by releasing earthquake source model constraints. Attenuation, site and transfer results are available from the authors. RMS residuals by phase and band are shown in Figure 4. Misfit is lower than for direct phases, with Lg coda best fit, followed by Pn and Sn, which are similarly

well fit. This latter is different than for direct phases, for which Pn is much more poorly fit than Sn. It is possible that the coda measurement has stabilized the Pn amplitude somewhat, although it is more likely that the limited region traversed by Pn in the coda study has decreased effects of mantle gradients and Moho fluctuations on Pn spreading. The behavior of Pn and Pn coda amplitudes remains an important research focus.

Resulting coda spectra for three events are shown in Figure 5. Results for the large earthquake show that spectra from different stations and coda types are consistent with each other. In general, Lg (and surface wave) coda allow us to estimate source spectra for lower bands, while Pn and Sn become important above 0.5 Hz. The best bands for Sn coda are slightly lower than the best bands for Pn coda. Results for the smaller event show that events exist for which no Lg coda can be measured, yet we can still estimate Mw. Results for the Indian test are included for interest's sake. Lg and Sn measures are consistent, while Pn is much higher, a well-known observation that allows the discrimination of this event for unusually low bands. Spectral fits for earthquake models are shown, as specified by standard MDAC methodology, but should not be taken seriously, as the low bands and Lg branch dominate the fit, and manual adjustment would be applied in such a situation.

CONCLUSIONS AND RECOMMENDATIONS

Absolute spectra from event cluster studies can be used in to constrain multi-band, multi-phase amplitude tomography to produce models that predict spectra from regional phase earthquake amplitudes. Further, absolute spectra can be used to validate propagation models in the same way that location ground truth is used to validate traveltimes models. Such models are critical for regional phase magnitude, yield and event identification analyses. In particular, source spectra derived from multiple coda types appear to be consistent between types and stations. Collection of absolute spectra must be a collaborative effort over time by the community, as has been the case for location ground truth.

ACKNOWLEDGMENTS

This study relied on IRIS and PASSCAL waveform collections, and we greatly appreciate help from IRIS DMC personnel. Graphics were made with GMT software. Valuable discussions with M. Fisk and K. Mayeda are gratefully acknowledged.

REFERENCES

- Campillo, M. (1987). Lg wave propagation in a laterally varying crust and the distribution of the apparent quality factor in central France, *J. Geophys. Res.* 92: 12,604–12,614.
- Fehler, M.C. and W.S. Phillips, Simultaneous inversion for Q and source parameters of microearthquakes accompanying hydraulic fracturing in granitic rock, *Bull. Seism. Soc. Am.*, **81**, 553-575, 1991.
- Fisk, M. and S. R. Taylor, (2007). Robust magnitude and path corrections for regional seismic phases in Eurasia by constrained inversion and enhanced kriging techniques, in *Proceedings of the 29th Monitoring Research Review: Ground-Based Nuclear Explosion Monitoring Technologies*, LA-UR-07-5613, Vol. 1, pp. 24–33.
- Ford, S.R., W.S. Phillips, W.R. Walter, M.E. Pasyanos, K.M. Mayeda, and D.S. Dreger (2009). Attenuation tomography of the Yellow Sea/Korean Peninsula from coda-source normalized and direct Lg amplitudes, *Pure Appl. Geophys.*, doi:10.1007/s00024-009-0023-2.
- Jin, A., and K. Aki (1988). Spatial and temporal correlation between coda-Q and seismicity in China, *Bull. Seismol. Soc. Am.* 78: 741–769.
- Malagnini, L., P. Bodin, K. Mayeda, A. Akinici (2006). Unbiased moment-rate spectra and absolute site effects in the Kachachh Basin, India, from the analysis of the aftershocks of the 2001 Mw 7.6 Bhuj earthquake, *Bull. Seismol. Soc. Am.* 96: doi:10.1785/0120050089.
- Mayeda, K.M., L. Malagnini, W.S. Phillips, W. Walter, and D. Dreger, (2005). 2-D or not 2-D, that is the question: A northern California test, *Geophys. Res. Lett.* 32: L12301, doi:10.1029/2005GL022882.
- Mayeda, K., L. Malagnini, W. R. Walter, (2007). A new spectral ratio method using narrow band coda envelopes: Evidence for non-self-similarity in the Hector Mine sequence, *Geophys. Res. Lett.*, doi:10.1029/2007GL030041.
- Mitchell, B. J., Y. Pan, J. Xu, and L. Cong (1997). Lg coda Q variation across Eurasia and its relation to crustal evolution, *J. Geophys. Res.* 102: 11767–22779.
- Nuttli O. W. (1973). Seismic wave attenuation and magnitude relations for eastern North America, *J. Geophys. Res.* 78: 876–885.

2011 Monitoring Research Review: Ground-Based Nuclear Explosion Monitoring Technologies

- Pasyanos, M.E., W.R. Walter, and E.M. Matzel (2009). A simultaneous multiphase approach to determine P-wave and S-wave attenuation of the crust and upper mantle, *Bull. Seismol. Soc. Am.* 99: 3314–3325.
- Pei, S., J. Zhao, C. A. Rowe, S. Wang, T. M. Hearn, Z. Xu, H. Liu, and Y. Sun (2006). M_L amplitude tomography in North China, *Bull. Seismol. Soc. Am.* 96: 1560–1566, doi: 10.1785/0120060021.
- Phillips, W. S., G. E. Randall and S. R. Taylor (1998). Path correction using interpolated amplitude residuals: An example from central China, *Geophys. Res. Lett.* 25: 2729–2732.
- Phillips, W. S., H. E. Hartse, S. R. Taylor, and G. E. Randall (2000a). 1 Hz Lg Q Tomography in central Asia, *Geophys. Res. Lett.* 27: 3425–3428.
- Phillips, W. S., H. E. Hartse, S. R. Taylor, A. A. Velasco, and G.E. Randall (2001). Application of regional phase amplitude tomography to seismic verification, *PAGEOPH*, 158: 1189–1206.
- Phillips, W. S., H. E. Hartse, and J. T. Rutledge (2005). Amplitude ratio tomography for regional phase Q, *Geophys. Res. Lett.* 32: doi:10.1029/2005GL023870.
- Phillips, W. S. and R. J. Stead (2008). Attenuation of Lg in the western US using the USArray, *Geophys. Res. Lett.* 35: L07307, doi:10.1029/2007GL032926.
- Phillips, W. S., R. J. Stead, G. E. Randall, H. E. Hartse, and K. Mayeda (2008). Source effects from broad area network calibration of regional distance coda waves, in *Advances in Geophysics, 50, Scattering of Short Period Waves in the Heterogeneous Earth*, H. Sato and M.C. Fehler, Eds., 319–351.
- Phillips, W.S., X. Yang, R.J. Stead, M.L. Begnaud, K.M. Mayeda (2010). Model development for broad area event identification and yield estimation, *Eos Trans. Am. Geophys. Union* 79: 4, 413–421.
- Taylor, S. R. (1996). Analysis of high frequency Pg/Lg ratios from NTS explosions and western US earthquakes, *Bull. Seismol. Soc. Am.* 86: 1042–1053.
- Taylor, S. R., X. Yang, and W. S. Phillips (2003). Bayesian Lg attenuation tomography applied to eastern Asia, *Bull. Seismol. Soc. Am.* 93: 795–803.
- Walter, W.R., K.M. Mayeda, and H.J. Patton, (1995). Phase and spectral ratio discrimination between NTS earthquakes and explosions: 1. Empirical observations, *Bull. Seismol. Soc. Am.* 85: 1050–1067.
- Walter, W. R. and S. R. Taylor (2002). A revised magnitude and distance amplitude correction (MDAC2) procedure for regional seismic discriminants: theory and testing at NTS, Lawrence Livermore National Laboratory, UCRL-ID-146882, pp. 13.
- Yang, X., T. Lay, X.-B. Xie, and M. S. Thorne (2007). Geometric spreading of Pn and Sn in a spherical Earth model, *Bull. Seism. Soc. Am.* 97: 6, 2053-2065.
- Xie, J. K., Z. Wu, R. Liu, D. Schaff, Y. Liu, and J. Liang (2006). Tomographic regionalization of crustal Lg Q in eastern Eurasia, *Geophys. Res. Lett.* 33: L03315, doi:10.1029/2005GL024410.

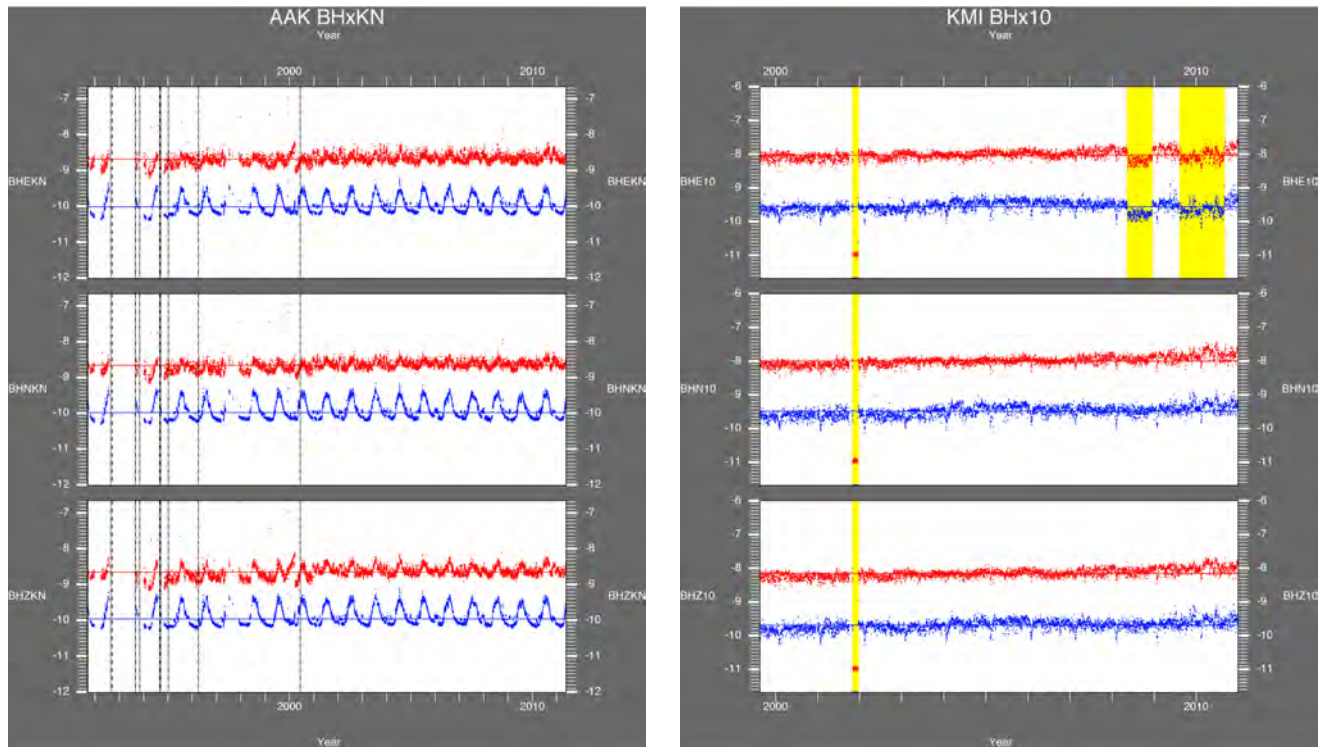


Figure 1. Nighttime noise versus time for bands 1-2 Hz (red) and 4-8 Hz (blue), for three components of stations AAK (left) and KMI (right). Noise amplitude units are \log_{10} displacement (m). 1-2 Hz amplitudes are shifted up one \log_{10} unit for display purposes. Known instrument response changes are marked by vertical lines. Yellow regions have been marked as “suspicious” and will not be used in amplitude studies without further review.

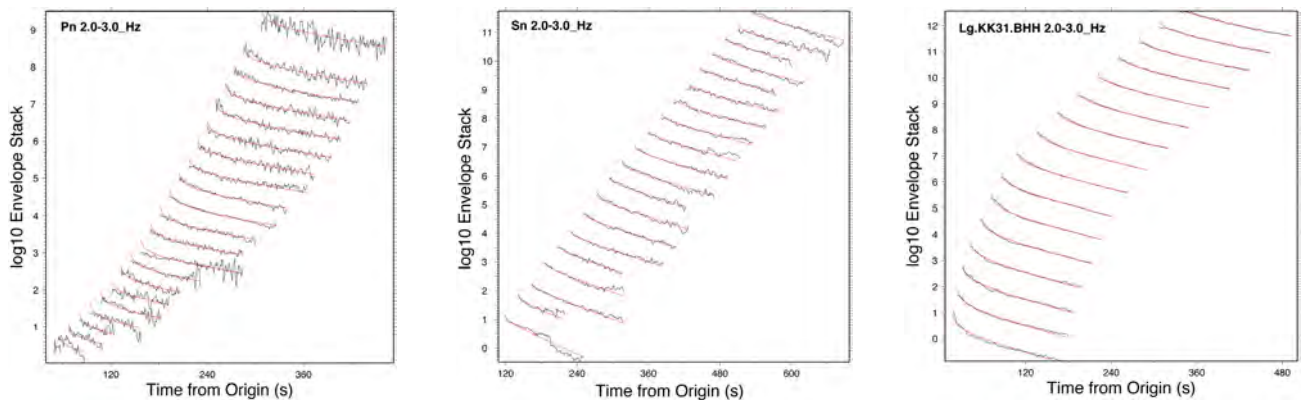


Figure 2. Coda shape functions for Pn (left), Sn (center) and Lg (right) for the 2-3 Hz band. Coda segments (black) represent stacks binned by distance range. Pn and Sn coda are network stacks, while the Lg coda are stacks for one station (KK31 horizontals). Each coda is shifted upwards from the previous distance bin by half of a \log_{10} unit for display purposes. The coda shape models based on simultaneous fit to all bands for each coda type are shown in red.

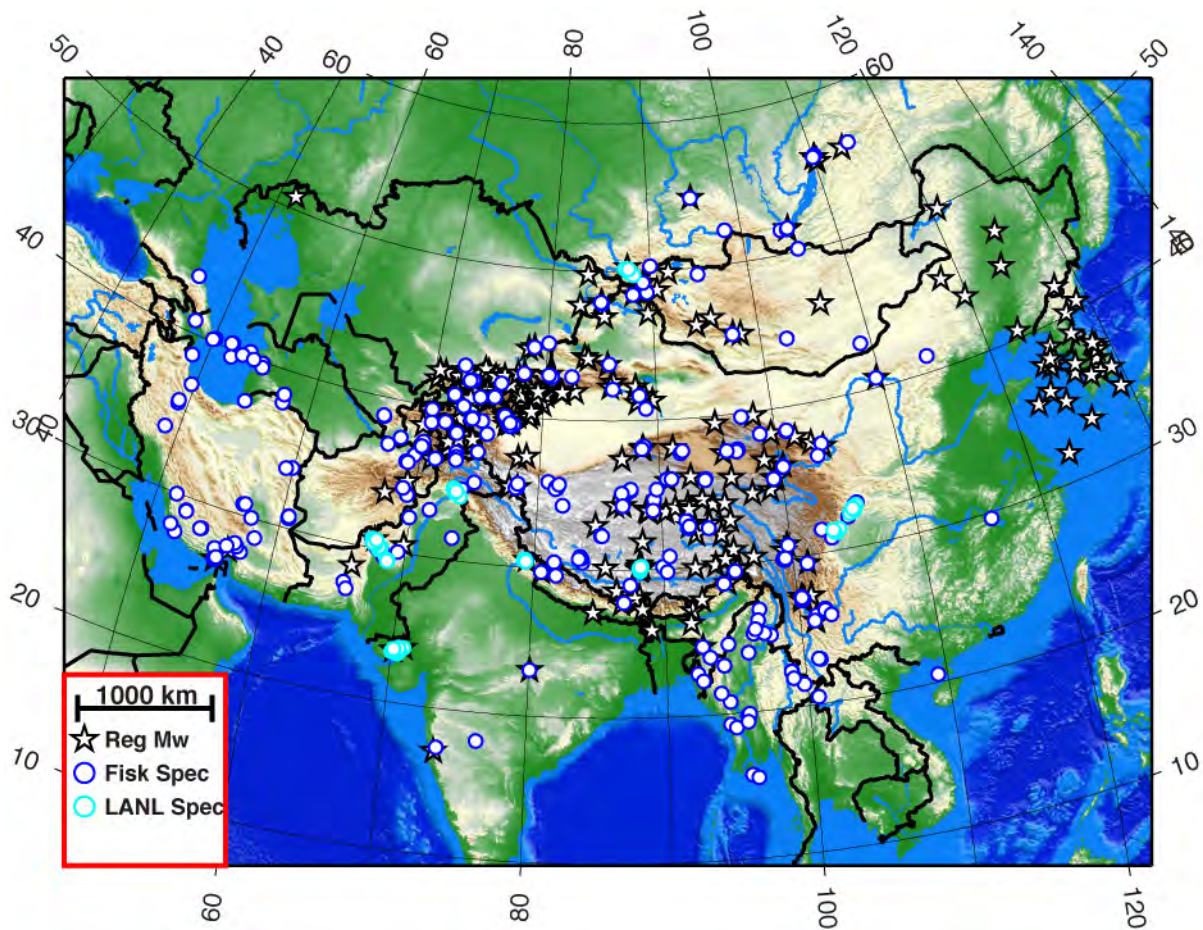


Figure 3. Events providing regional moments (stars) and spectral constraints (circles) to the coda path inversion. Moments have been collected by LANL and LLNL, most from the literature and previous BAA contracts. Spectral constraints have been provided by M. Fisk (blue) and computed at LANL (cyan) by applying relative direct and coda wave techniques to event clusters.

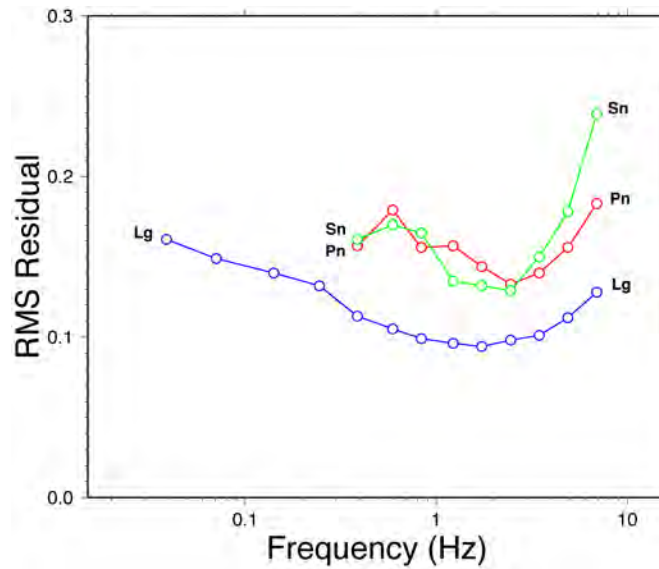


Figure 4. RMS \log_{10} amplitude residuals for path-site-transfer function inversion for three coda types versus frequency.

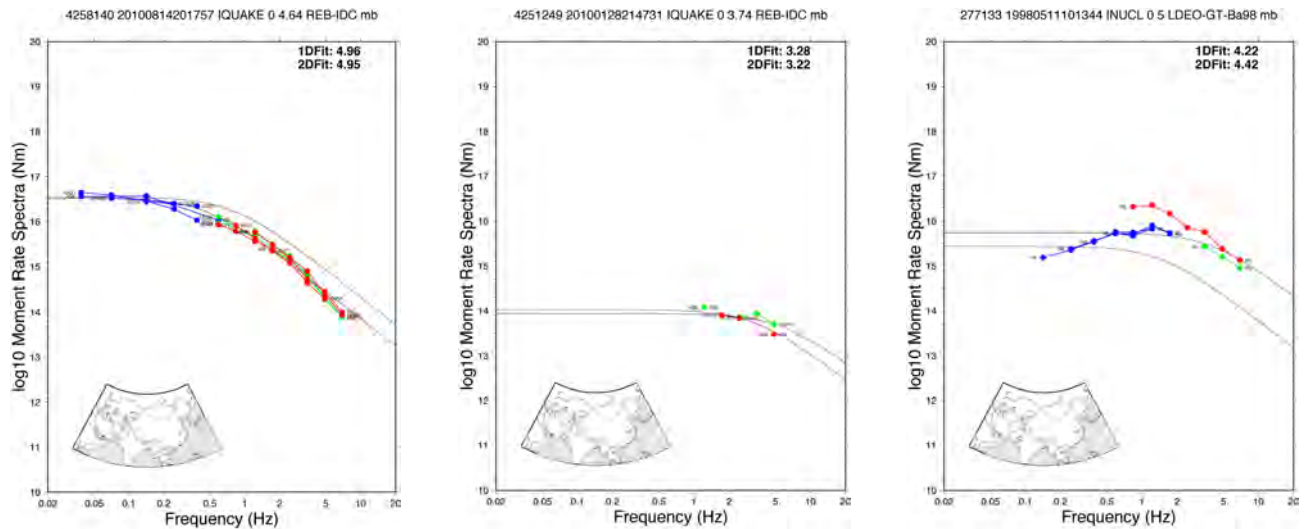


Figure 5. Coda spectra for large (left) and small (center) earthquakes, and for the 1998 Indian test (right). Lg (blue), Sn (green) and Pn (red) coda types are shown. Multiple stations are used; results for individual stations are connected and annotated at high and low band endpoints. Moments and spectra for 1-D and 2-D fits of the omega-squared source model are shown. 1-D fits are constrained by a constant stress scaling model, while 2-D fits allow the corner frequency (or stress) free. Fits are weighted heavily towards low bands. Note that the automated L1 fitting routine chose the Lg and Sn spectra for the Indian test, even though the Pn results would be more appropriate. MDAC discrimination procedures call for all events to be fit by an earthquake model, as the source type is assumed unknown. Further, results capture the unusually large difference between 1 Hz P and S spectra noted by previous authors for this test.